The Kinetic Mechanism of AAC(3)-IV Aminoglycoside Acetyltransferase from *Escherichia coli*†

Maria L. B. Magalhaes and John S. Blanchard*

Department of Biochemistry, Albert Einstein College of Medicine, 1300 Morris Park Avenue, Bronx, New York 10461

Received September 2, 2005; Revised Manuscript Received October 18, 2005

ABSTRACT: The aminoglycoside 3-*N*-acetyltransferase AAC(3)-IV from *Escherichia coli* exhibits a very broad aminoglycoside specificity, causing resistance to a large number of aminoglycosides, including the atypical veterinary antibiotic, apramycin. We report here on the characterization of the substrate specificity and kinetic mechanism of the acetyl transfer reaction catalyzed by AAC(3)-IV. The steady-state kinetic parameters revealed a narrow specificity for the acyl-donor and broad range of activity for aminoglycosides. AAC(3)-IV has the broadest substrate specificity of all AAC(3)'s studied to date. Dead-end inhibition and ITC experiments revealed that AAC(3)-IV follows a sequential, random bi-bi kinetic mechanism. The analysis of the pH dependence of the kinetic parameters revealed acid- and base-assisted catalysis and the existence of three additional ionizable groups involved in substrate binding. The magnitude of the solvent kinetic isotope effects suggests that a chemical step is at least partially rate limiting in the overall reaction.

Aminoglycoside antibiotics are used in the treatment of a variety of diseases caused by both Gram-positive and Gram-negative bacterial infections (*1*), acting primarily by impairing bacterial protein synthesis as a result of binding to the A (acceptor) site of the 30S prokaryotic ribosome (*2*). The clinical use of these drugs in the 1960s and 1970s led to the appearance of resistant strains (*1*). The most clinically important mechanism of aminoglycoside resistance is the decreased affinity of the drug for its target after enzymatic modification (*3*). Aminoglycoside acetyltransferases catalyze the AcCoA-dependent[1] *N*-acetylation of amino groups (Scheme 1) on aminoglycoside molecules (Figure 1) (*4*). The AAC(3) family of aminoglycoside acetyltransferases regioselectively modify the 3-amino group of the deoxystreptamine ring, and this family includes four types, I−IV, based on the pattern of aminoglycoside resistance that they confer (*4*). The AAC(3)-I and -II isoenzymes preferentially modify the gentamicin group of aminoglycosides (*5*, *6*). AAC(3)-III enzymes catalyze the covalent acetylation of a wide variety of aminoglycosides including gentamicin, tobramycin, and neomycin (*7*).

The AAC(3)-IV class of *N*-acetyltransferases have the broadest substrate specificity of all AAC(3) enzymes identified to date, and also acetylate the atypical aminoglycoside apramycin (Scheme 1) (*8*). Apramycin was first approved for veterinary use in the United States in the 1980s. It was thought that the unusual structure of apramycin, including the fused central rings and terminal deoxystreptamine ring compared to the central deoxystreptamine ring of the typical aminoglycosides, might prevent its inactivation by known aminoglycoside-modifying enzymes, and thus would not interfere with the clinical usefulness of other typical disubstituted deoxystreptamine aminoglycosides (Figure 1). However, enterobacteria of animal origin were found to be resistant to apramycin by the expression of a plasmid-encoded AAC(3)-IV enzyme (*9*). Following the rapid spread of the apramycin resistance gene (*aacC4*) in animals, the plasmid was later found in clinical isolates from hospitalized patients (*10*). The broad substrate activity of AAC(3)-IV and the presence of the plasmid in human clinical isolates represents a serious therapeutic concern, since essentially all aminoglycosides used in human antibiotic therapy are substrates for this enzyme.

In the study reported here, we have cloned and overexpressed the plasmid encoded AAC(3)-IV enzyme from *Escherichia coli*. We have studied the substrate specificity of AAC(3)-IV for various aminoglycosides and CoA thioester analogues and determined the kinetic mechanism of this enzyme. The determination of the solvent kinetic isotope effects and pH dependence of the kinetic parameters provided some insights into the chemical mechanism of the enzyme.

MATERIALS AND METHODS

Materials. Restriction enzymes and T4 DNA ligase were from New England Biolabs. *Pfu* DNA polymerase was from Stratagene. The pET23a(+) expression vector and *E. coli* BL21(DE3) pLysS were from Novagen. All chromatographic supports were from Pharmacia. Aminoglycosides, acyl-coenzymes A, and 4,4′-dithiodipyridine (DTDP) were purchased from Sigma Chemical Co. The *aacC*4 gene was

† This work was supported by NIH Grant AI60899.

* Corresponding author. Tel: (718) 430-3096. Fax: (718) 430-8565. E-mail: blanchar@aecom.yu.edu.

[1] Abbreviations: AAC(3), 3-*N*-aminoglycoside acetyltransferase; AMP, adenosine monophosphate; AcCoA, acetyl-coenzyme A; CoA, coenzyme A; DTDP, 4,4′-dithiodipyridine; GNAT, GCN5-related *N*-acyltransferase; HEPES, N-[2-hydroxyethyl] piperazine-N′-[2-ethanesulfonic acid]; Iptg, isopropyl-thio-β-D-galactopyranoside; ITC, isothermal titration calorimetry; KIE, kinetic isotope effect; LB, Luria broth; PCR, polymerase chain reaction; SDS−PAGE, sodium dodecyl sulfate−polyacrylamide gel electrophoresis; TEA, triethanolamine.

10.1021/bi051777d CCC: $30.25 © 2005 American Chemical Society
Published on Web 11/16/2005

Scheme 1: Reaction Catalyzed by *E. coli* AAC(3)-IV

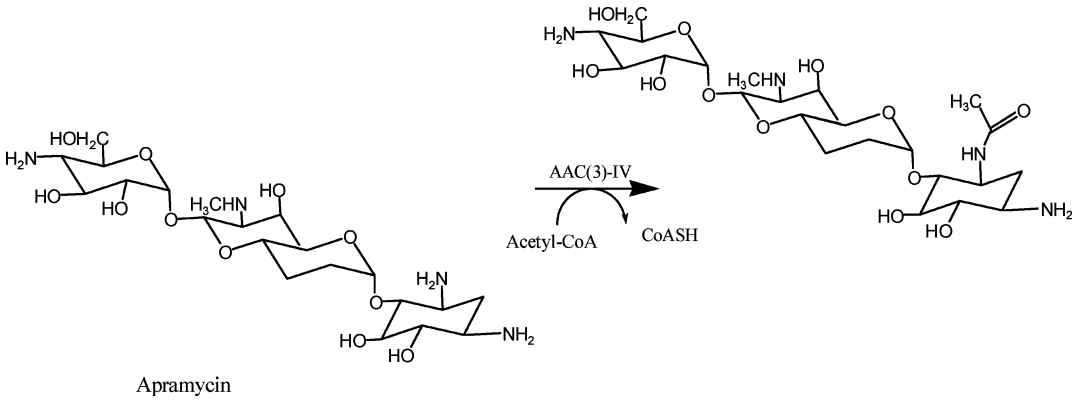

Apramycin

contained on plasmid pMP139 (a kind gift of Dr. Martin S. Pavelka Jr., University of Rochester School of Medicine and Dentistry).

Cloning and Expression of the E. coli aacC4 Gene. Synthetic oligonucleotide primers (5′ acatatgcaatacgaatggcgaaaagcc 3′ and 5′ aaagctttcatgagctcagccaatcgac 3′) were used to amplify the *E. coli aacC4* gene (786 bp) from plasmid pMP139 (*11*) using standard PCR conditions and *Pfu* DNA polymerase. These primers are complementary to the 5′ and 3′ ends of *aacC4* gene and introduce unique *Nde*I and *Hin*dIII restriction enzyme sites, respectively (underlined). The fragment was inserted into an *Nde*I−*Hin*dIII digested pET23a(+) expression vector. The recombinant plasmid pET23a(+)::*aacC4* was transformed into competent *E. coli* BL21(DE3) pLysS cells. The transformed cells were inoculated into LB media containing 50 μg/mL carbenicillin and were grown at 37 °C for 24 h. Control experiments were performed with *E. coli* cells containing just pET23(a)+ and lacking the target gene. Protein concentrations were determined by the method of Bradford (*12*) using the Bio-Rad protein assay kit and bovine serum albumin as standard.

Purification of AAC(3)-IV. All protein purification procedures were carried out at 4 °C. The purity of AAC(3)-IV was analyzed by SDS−PAGE on a Phast System (Pharmacia). Ten grams of cells was suspended in 50 mL of 20 mM triethanolamine hydrochloride (TEA), pH 7.8 (buffer A), containing protease inhibitor cocktail (Roche) and DNAse I (5 μg/mL). The cells were disrupted by sonication and stirred on ice for 30 min. The cell debris was removed by centrifugation for 45 min at 11 000 rpm. The supernatant was applied to a 140 mL Fast Flow Q-Sepharose anion-exchange column preequilibrated with buffer A, and proteins were eluted with a linear gradient from 0 to 0.5 M NaCl. Active fractions were pooled and dialyzed against buffer A, and $(NH_4)_2SO_4$ was added to a final concentration of 1 M. After centrifugation to remove insoluble material, the supernatant was applied to a 140 mL Phenyl Sepharose column preequilibrated with buffer C (20 mM TEA, pH 7.8, 1 M $(NH_4)_2SO_4$). Proteins were eluted with a linear 1−0 M $(NH_4)_2SO_4$ gradient. The active fractions were pooled and dialyzed against buffer A. These fractions exhibited a single band on SDS−PAGE with Coomassie Blue staining.

Protein Analysis. Analytical gel filtration experiments were performed with a Sephacryl-S200 gel filtration column, calibrated using Bio-Rad molecular weight markers, in 20 mM TEA pH 7.8. Dynamic light scattering was measured with a DynaPro MS/X dynamic light-scattering instrument (Protein Solutions) with samples of AAC(3)-IV at 15 mg/mL.

Measurement of Enzyme Activity. Aminoglycoside-dependent acetyltransferase activity was monitored spectrophotometrically by following the increase in absorbance at 324 nm due to the reaction between the sulfhydryl group of the product CoASH and DTDP, releasing 4-thiopyridone (ϵ_{324} = 19 800 M^{-1} cm^{-1}). Reactions were monitored continuously on a UVIKON 943 spectrophotometer, and enzyme activities were calculated from the initial (<10% completion) rates. Assay mixtures contained 50 mM HEPES, pH 7.5 and 0.1 mM DTDP, in addition to enzyme, substrate, and inhibitors in a final volume of 1 mL. Reactions were initiated by the addition of enzyme and followed at 25 °C.

Initial Velocity Experiments. Initial velocity kinetic data were fitted using Sigma Plot 2000. A plot of steady-state velocity vs enzyme concentration was linear over the concentration range used and passes through the origin. Substrate specificity of AAC(3)-IV was determined at pH 7.5 at 10 different concentrations of the variable substrate and a fixed, saturating concentration ($10K_m$−$15K_m$) of the second substrate. Kinetic constants for acetyl-CoA and other CoA-derivatives were determined at fixed saturating concentration ($15K_m$) of apramycin, while the constants for the aminoglycosides were determined using fixed saturating concentrations ($10K_m$−$15K_m$) of acetyl-CoA. Individual substrate saturation kinetic data were fitted to eq 1.

$$v = VA/(K_a + A) \quad (1)$$

Initial velocity patterns were obtained by measuring the initial rate at five concentrations of each substrate. Equation 2 was used to fit the intersecting initial velocity pattern.

$$v = VAB/(K_aB + K_bA + K_{ia}K_b + AB) \quad (2)$$

Dead-End Inhibition Patterns. Dead-end inhibition patterns were determined by measuring initial velocities at variable concentrations of one reactant, the second reactant concentration fixed at its K_m value, and the inhibitor at several concentrations. Equations 3 and 4 were used to fit linear competitive and noncompetitive inhibition data, respectively.

$$v = VA/[K_a(1 + I/K_{is}) + A] \quad (3)$$

$$v = VA/[K_a(1 + I/K_{is}) + A(1 + I/K_{ii})] \quad (4)$$

Structures of 4,5-Substituted Aminoglycoside Antibiotics

A

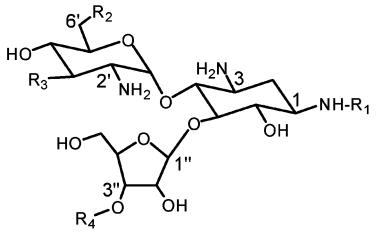

Antibiotic	R_1	R_2	R_3	R_4
Ribostamycin	H	NH_2	OH	H
Butirosin	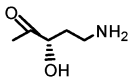	NH_2	OH	H
Paromomycin	H	OH	OH	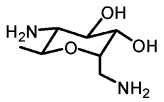
NeomycinB	H	NH_2	OH	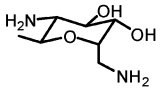

B Structures of 4,6-Disubstituted Aminoglycoside Substrates

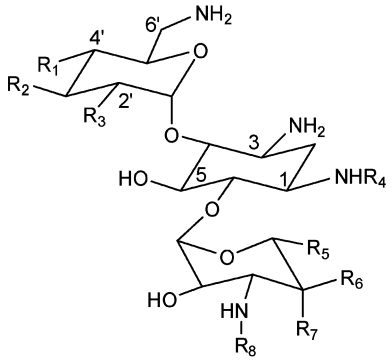

Antibiotic	R_1	R_2	R_3	R_4	R_5	R6	R7	R8
Tobramycin	OH	H	NH_2	H	CH_2OH	OH	H	H
Kanamycin A	OH	OH	OH	H	CH_2OH	OH	H	H
Amikacin	OH	OH	OH	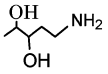	CH_2OH	OH	H	H
Gentamycin C1	H	H	NH_2	H	H	CH_3	OH	CH_3
Sisomicin*	H	H	NH_2	H	H	CH_3	OH	CH_3
Netilimicin*	H	H	NH_2	CH_2CH_3	H	CH_3	OH	CH_3

* (Δ5'>4' unsaturation)

FIGURE 1: Structures of 4,5-disubstituted (A) and 4,6-disubstituted (B) aminoglycosides used in this study. Because of its unusual structure, apramycin is not represented here, but in Scheme 1.

In eqs 1−4, v is the measured reaction velocity, V is the maximal velocity, A and B are the concentrations of the substrates (aminoglycoside and acyl-CoA, respectively), K_a and K_b are the corresponding Michaelis−Menten constants, K_{ia} is the inhibition constant for substrate A, I is the concentration of inhibitor, and K_{is} and K_{ii} are the slope and the intercept inhibition constant for the inhibitor, respectively.

Equation 5 was used to fit kinetic plots in which "substrate activation" was apparent from Lineweaver−Burk plots, where v is the measured reaction velocity, V is the maximal velocity, and A is the concentration of the variable substrate. The constants B, C, and D are collections of rate constants that depend on the kinetic mechanism and the resulting rate equation. Equation 6 was used to fit kinetic plots in which

$$v = V(A^2 + DA)/(A^2 + BA + C) \quad (5)$$

"substrate inhibition" was apparent from Lineweaver−Burk plots, where v is the measured reaction velocity, V is the maximal velocity, A is the concentration of the variable substrate, and K and K_i are the corresponding Michaelis−Menten and inhibition constant for substrate A, respectively.

$$v = (VA)/K + A + (A^2/K_i) \quad (6)$$

Dependence of pH on AAC(3)-IV Activity. pH studies on AAC(3)-IV were performed to generate a profile of enzyme activity as a function of pH. Ribostamycin was used as the variable substrate. Acetyl transfer activity was monitored from pH 5.4 to 9.9 every 0.5 pH unit using the following buffers: MES (pH 5.4−6.5), HEPES (pH 6.5−8.0), or CHES (pH 8.0−10.0). The resulting kinetic data were fitted to eq 1 to obtain the kinetic parameters: k_{cat} and k_{cat}/K_m. Profiles were generated by plotting the log of k_{cat} or k_{cat}/K_m versus the pH and fitted using eqs 7 and 8. Equation 7 describes

$$v = C/(1 + H/K_a + K_b/H) \quad (7)$$

$$v = C/(1 + (H^2/K_a^2) + (K_b^3/H^3)) \quad (8)$$

one acidic and one basic pK_a value, while eq 8 assumes two acidic and three basic pK_a values. C is the pH-independent plateau value, H is the hydrogen ion concentration, and K_a and K_b are the respective acidic and basic pK_a constants for the ionizing groups.

Solvent Kinetic Isotope Effects. The solvent kinetic isotope effects on k_{cat} and k_{cat}/K_m were determined by measuring the initial velocities using saturating concentrations of acetyl-CoA and variable concentrations of ribostamycin in either H_2O or 90% D_2O at pH 8.0.[2] Solvent deuterium kinetic isotope effects were fitted to eq 9. Equation 9 assumes equivalent effects on both k_{cat} and k_{cat}/K_m, where v is the measured reaction velocity, V is the maximal velocity, A is the concentration of the substrate, K_a is the Michaelis constant for the substrate whose concentration is being varied, F_i is the fraction of the heavy atom, and E_{KIE} is the isotope effect.

$$v = VA/(K_a + A)[1 + F_i(E_{KIE} - 1)] \quad (9)$$

Isothermal Titration Calorimetry. ITC experiments were performed using a VP-ITC microcalorimeter from Microcal, Inc. (Northampton, MA). All measurements were carried out at 27 °C in 50 mM Tris buffer pH 7.5. Enzyme preparations were dialyzed extensively against the above buffer, and all ligand solutions were prepared in the final dialysate. In individual titrations, injections of 5 μL of either acetyl-CoA (5mM) or ribostamycin (10 mM) were made into the enzyme solution (cell volume = 1.43 mL) via a computer-controlled microsyringe, at an interval of 4 min, while being stirred at 310 rpm. The instrument was calibrated using the calibration kit supplied by the manufacturer. The quantity $c = K_aM_t(0)$, where $M_t(0)$ is the initial macromolecule concentration, is of importance in titration microcalorimetry (*13*). All experiments were performed with c values in the range of 2−100 in the present study. The experimental data were fitted to a theoretical titration curve using software supplied by Microcal, with ΔH (the binding enthalpy change in kcal mol^{-1}), K_a (the binding constant in M^{-1}), and n (the number of binding sites per monomer) as adjustable parameters. The thermodynamic parameters ΔG and ΔS were calculated from eq 10,

$$\Delta G = \Delta H - T\Delta S = -RT \ln K_a \quad (10)$$

where ΔG, ΔH, and ΔS are the changes in free energy, enthalpy, and entropy of binding. T is the absolute temperature, and $R = 1.98$ cal mol^{-1} K^{-1}.

RESULTS

Cloning, Expression, and Purification of AAC(3)-IV. PCR amplification of the *E. coli aacC4* gene using the plasmid pMP139 (*11*) as DNA template yielded a fragment of the expected length. The fragment was cloned into the pET23a-(+) expression vector, and the *aacC4* structural gene was sequenced to ensure its identity, and that no mutations were introduced during the amplification step. However, the sequencing of several independent clones showed the absence of a cytosine at position 732 when compared to the *aacC4* gene sequence deposited in GenBank. Sequence analysis of the original plasmid pMP139 by Dr. Martin S. Pavelka, Jr. (University of Rochester), confirmed the absence of C732. The absence of C732 alters the reading frame, introduces a stop codon, and reduces the protein from 261 to 258 amino acids. This sequence has been submitted to GenBank with accession code DQ241380. *E. coli* strain BL21(DE3) pLysS containing the plasmid pET23(a)+::*aacC4* expressed approximately 50 mg of soluble AAC(3)-IV per liter of culture, with an apparent molecular weight, by SDS−PAGE, in agreement with the predicted value of 27 874 deduced from corrected nucleotide sequence. This protein product was absent in control experiments where only the plasmid pET23-(a)+ was expressed in *E. coli* BL21(DE3)pLysS. The highest protein yield was obtained from cells grown for 24 h at 37 °C with no addition of the inducer IPTG. The two-step purification procedure yielded greater than 95% pure protein and catalytically active AAC(3)-IV enzyme. Analytical gel filtration over a Sephacryl-S200 column revealed a single peak of ca. 60 kDa, which corresponds to a dimer of 28 kDa monomers in solution. This result was confirmed by dynamic light scattering experiments, where the major peak represents a macromolecule of 54 kDa (data not shown).

Substrate Specificity of AAC(3)-IV. The steady-state kinetic parameters for AcCoA and other CoA derivatives at saturating concentrations (15K_m) of apramycin are summarized in Table 1. AcCoA is the best substrate on the basis of the k_{cat}/K_m values and was used as the acyl-donor in subsequent experiments. The kinetic parameters of various aminoglycosides, determined at saturating concentrations (10K_m−15K_m) of AcCoA, are also summarized in Table 1. The structures of aminoglycosides used are shown in Figure 1. Aminoglycosides can be separated into three groups on the basis of their kinetic behavior. Amikacin, apramycin, and kanamycin A exhibited linear double-reciprocal plots. Butirosin, gentamycin, neomycin, paromomycin, tobramycin, and sisomycin exhibited linear kinetics at low substrate concentration but rapidly increasing reaction velocities at higher aminoglycoside concentrations. This phenomenon, termed substrate activation, has previously been observed with other aminoglycoside acetyltransferases (*14*, *15*). For substrates exhibiting this phenomenon, two pairs of fitted kinetic constants are included in Table 1. On average, k_{cat}^2 was 0.8 times higher than k_{cat}, K_m^2 was 10 times higher than

[2] Solvent kinetic isotope effects were measured by preparing a 10 times concentrated solution of buffer and substrates in 100 μL. To these concentrated reaction mixtures was added 900 μL of either H_2O or D_2O. Experiments were repeated in triplicate, and the average of the initial velocities at each substrate determination was used to determine the isotope effect (Figure 4). The pH meter readings of the mixtures after the initial velocity was determined were 7.92 and 8.07 for H_2O and 90% D_2O reaction mixtures, respectively.

Table 1: Kinetic Parameters for AAC(3)-IV

substrate	K_m (μM)	k_{cat} (s^{-1})	k_{cat}/K_m (M^{-1} s^{-1})	$K_m{}^2$ (μM)	$k_{cat}{}^2$ (s^{-1})	$k_{cat}/K_m{}^2$ (M^{-1} s^{-1})
A[c]						
acetyl-CoA	86 ± 6	39 ± 1	4.5×10^5			
propionyl-CoA	499 ± 90	33 ± 2	6.6×10^4			
malonyl-CoA	477 ± 80	9 ± 1	1.9×10^4			
butyryl-CoA	1160 ± 70	0.30 ± 0.01	2.6×10^2			
B[d]						
neomycin[a]	0.36 ± 0.03	60 ± 9	1.6×10^8	1.4 ± 0.3	80 ± 4	5.7×10^7
sisomycin[a]	0.33 ± 0.02	51 ± 1	1.5×10^8	2.5 ± 0.4	72 ± 2	2.8×10^7
tobramycin[a]	1.42 ± 0.05	162 ± 4	1.1×10^8	7.3 ± 0.9	245 ± 13	3.3×10^7
parmomycin[a]	0.15 ± 0.01	15.0 ± 0.1	1.0×10^8	2.2 ± 0.5	24 ± 2	1.1×10^7
apramycin	0.67 ± 0.07	61 ± 1	9.1×10^7			
ribostamycin[b]	3.1 ± 0.3	146 ± 4	4.6×10^7			
gentamycin[a]	0.97 ± 0.02	40 ± 3	4.1×10^7	22 ± 4	90 ± 6	4.1×10^6
netilmicin[b]	42 ± 7	32 ± 2	7.6×10^5			
kanamycin A	238 ± 36	80 ± 2	3.4×10^5			
butirosyn[a]	237 ± 17	3.5 ± 0.2	1.5×10^4	1368 ± 23	9 ± 2	6.6×10^3
amikacin	1107 ± 144	0.50 ± 0.03	4.5×10^2			

[a] Substrate exhibiting substrate activation. [b] Substrate exhibiting substrate inhibition. [c] Determined at fixed, saturating concentration ($15K_m$) of apramycin. [d] Determined at fixed, saturating concentration ($10K_m-15K_m$) of acetyl-CoA.

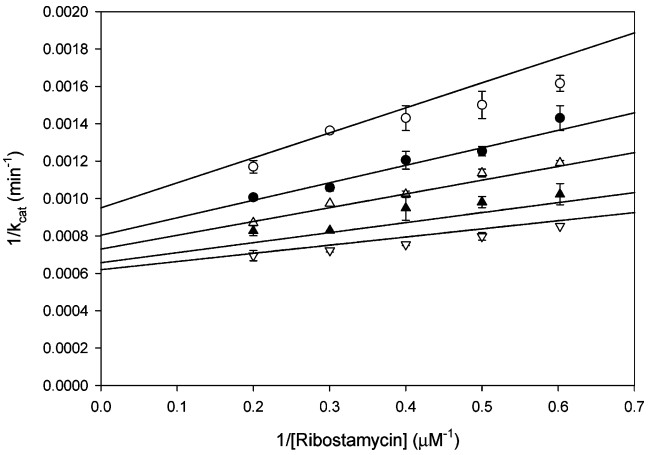

FIGURE 2: Double reciprocal plot of initial rate data at varying ribostamycin concentrations and fixed concentrations of AcCoA at 5 μM (○), 7.5 μM (●), 10 μM (△), 15 μM (▲), and 20 μM (▽).

K_m, and $k_{cat}/K_m{}^2$ was 10 times lower than k_{cat}/K_m. The third group includes netilmicin and ribostamycin, which exhibited linear kinetics at low substrate concentration but rapidly decreasing reaction velocities at higher aminoglycoside concentrations. This phenomenon is referred to as substrate inhibition and has also been observed with other aminoglycoside acetyltransferases (*16*, *17*). Amikacin, butirosin, and netilmicin, which are 1-*N*-substituted derivatives of kanamycin A, ribostamycin, and sisomycin, respectively, are poor substrates, based on their k_{cat}/K_m values, when compared to their nonsubstituted derivatives.

Kinetic Mechanism. To determine the kinetic mechanism and distinguish between a ternary complex and a ping-pong mechanism, steady-state initial velocities were determined using five different concentrations of both AcCoA and ribostamycin. Ribostamycin was chosen for these studies due to its rapid acetylation and its K_m value that allows for acquisition of high quality initial rate data. However, it was used in a limited concentration range ($0.5K_m-1.5K_m$), since substrate inhibition is observed at higher concentrations. Analysis of the resultant double reciprocal plot (Figure 2) revealed an intersecting pattern, indicating the formation of a ternary E−AcCoA−ribostamycin complex. Several distinct kinetic mechanisms are possible for enzymes systems that employ two substrates and generate two products, including random, fully ordered, or a combination of both. Dead-end inhibition studies can distinguish among the various possibilities. Butirosin, which differs from ribostamycin only by a substitution in the 1-*N* position of the deoxystreptamine ring, is an extremely poor substrate for AAC(3)-IV and a potent inhibitor of the enzyme. Experiments were carried out using butirosin, as inhibitor, versus either ribostamycin or AcCoA. Butirosin exhibited linear competitive inhibition versus ribostamycin and linear, noncompetitive inhibition versus AcCoA (Table 2, Figure S2A, B (Supporting Information). Desulfocoenzyme A is a coenzyme A derivative which lacks the terminal sulfhydryl of CoA and is a dead-end inhibitor since it forms a nonproductive complex with AAC(3)-IV and the aminoglycoside. Desulfocoenzyme A exhibited a linear, competitive inhibition versus AcCoA and linear, noncompetitive inhibition versus ribostamycin (Table 2, Figure S2C, D).

Isothermal Titration Calorimetry. We employed ITC studies to investigate the binding of AcCoA and ribostamycin to AAC(3)-IV (Figure S5, Supporting Information). The thermodynamic binding parameters are presented in Table 3. The titration with AcCoA resulted in an experimental K_d of 5 ± 0.1 μM, $-\Delta H$ value of 9.1 kcal mol^{-1}, and $-T\Delta S$ of 1.9 kcal mol^{-1}. The titration with ribostamycin resulted in a 10-fold higher K_d of 55 ± 4 μM when compared to AcCoA. The enthalpic and entropic contribution upon binding of ribostamycin also appeared to be quite distinct from AcCoA, with a $-\Delta H$ value of 0.67 kcal mol^{-1} and $-T\Delta S$ value of -5.13 kcal mol^{-1}. The ITC data also demonstrated that there is one substrate-binding site per AAC(3)-IV monomer.

Dependence of pH on AAC(3)-IV Activity. pH studies were performed to investigate the ionization behavior of groups responsible for catalysis and binding. The pH dependence of k_{cat} reveals both acid- and base-assisted catalysis. The bell-shaped plot of the log of k_{cat} versus pH has slopes of $+1$ and -1 in the acidic and basic regions, respectively (Figure 3), indicative of acid/base catalysis. The group that must be deprotonated for catalysis exhibits a pK_a value of 7.8 ± 0.2 and the group that must be protonated for catalysis exhibits

Table 2: Summary of AAC(3)-IV Dead-End Inhibition Studies

inhibitor	varied substrate	fixed substrate	pattern of inhibition	K_{is} (μM)	K_{ii} (μM)
desulfo-CoA	acetyl-CoA	paromomycin (10μM)	competitive	9 ± 1	
desulfo-CoA	ribostamycin	acetyl-CoA (40μM)	noncompetitive	90 ± 26	56 ± 8
butirosin	acetyl-CoA	ribostamycin (20μM)	noncompetitive	111 ± 30	54 ± 6
butirosin	ribostamycin	acetyl-CoA (500μM)	competitive	1.4 ± 0.1	

Table 3: Thermodynamic Parameters Obtained from Calorimetric Titration of AAC(3)-IV[a]

ligand	K_a ($\times 10^4$ M^{-1})	$-\Delta G$ (kcal mol^{-1})	$-\Delta H$ (kcal mol^{-1})	$-T\Delta S$ (kcal mol^{-1})
AcCoA	19.8	7.2	9.1	1.9
ribostamycin	1.8	5.8	0.67	−5.13

[a] Determined at 300 K. Relative error values: K_a, 1−6%; ΔH, 1−4%.

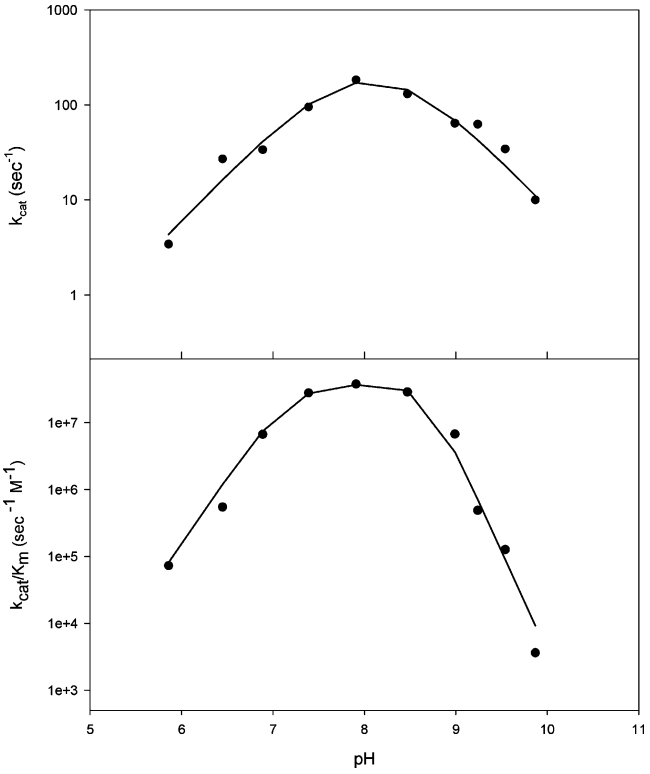

FIGURE 3: pH profiles of AAC(3)-IV activity as function of pH. The symbols are experimentally determined values, while the lines are fits of the data to eqs 7 and 8. The ascending curve on log k_{cat} plot shows that one ionizable group (pK_a 7.8 $\pm$ 0.2) must be deprotonated for optimal catalytic efficiency. The descending curve represents an ionizable group with a pK_a value of 8.4 $\pm$ 0.2, which must be protonated for optimal activity. The slopes of +2 in the acidic region and −3 in the basic region of k_{cat}/K_m plot reveals three additional groups involved in substrate binding.

a pK_a value of 8.4 $\pm$ 0.2. The plot of k_{cat}/K_m for ribostamycin versus pH is also bell-shaped, with slopes of +2 in the acidic region and −3 in the basic region, which suggests three additional groups on ribostamycin or enzyme involved in substrate binding. The acidic groups exhibit nonresolvable pK_a values of 7.2 $\pm$ 0.1, while those in the basic region exhibit nonresolvable pK_a values of 8.7 $\pm$ 0.1.

Solvent Kinetic Isotope Effects. Solvent kinetic isotope effects were performed at pH 8.0 in either H_2O or 90% D_2O.[2] This pH was chosen because it corresponds to the plateau region of the pH profile, where the velocity is maximal and the variations in velocity due to changes in pH are smallest. Ribostamycin was tested as the variable substrate, and

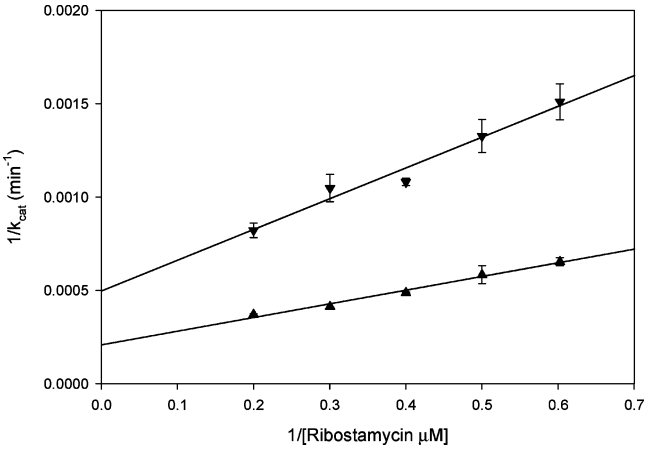

FIGURE 4: Solvent kinetic isotope effect determined for AAC(3)-IV. The symbols are the experimentally determined values in H_2O (▲) or 90% D_2O (▼), while the lines are fits of the data to eq 9. Ribostamycin was the variable substrate, and AcCoA was present at saturating concentrations.

reactions were performed at fixed, saturating concentrations of AcCoA (Figure 4). Ribostamycin exhibited identical effects of 2.5 $\pm$ 0.1 for both $^{D2O}k_{cat}$ and $^{D2O}k_{cat}/K_m$.

DISCUSSION

The sequencing of the PCR product of the *aacC4* gene contained on the plasmid pMP139 (*11*) showed the absence of a cytosine in the position 732. Several clones were analyzed, however, in all clones tested the absence of C732 was observed. Additional sequence analysis of the original plasmid (Dr. Martin S. Pavelka, Jr., University of Rochester) confirmed the *minus C-732* sequence as correct, and the sequence deposited in GenBank (accession number AJ438947) is incorrect. This deletion changes the reading frame at the very end of the gene, introducing a stop codon and reducing the protein length from 261 to 258 amino acids. The new sequence also changes the subunit molecular weight from 28 459 to 27 874 as well as the predicted isoelectric point from 6.38 to 5.66. Previous studies with AAC(3)-IV reported an isoelectric point of 5.6 (*18*), in accordance with the correct protein sequence.

Protein sequence analysis showed significant similarity between AAC(3)-IV and aminoglycoside 3-*N*-acetyltransferases types II and III from several organisms, none of which have been structurally characterized. AAC(3)-Ia from *Serratia marcescens* is the only aminoglycoside 3-*N*-acetyltransferases whose structure has been determined, and is a member of the GCN5-related *N*-acetyltransferase (GNAT) superfamily (*19*). AAC(3)-IV did not show any sequence similarity to AAC(3)-Ia or any other member of the GNAT family, strongly suggesting that AAC(3)-IV does not share the same fold.

The *E. coli aacC4* gene was cloned into the pET-23a(+) expression vector, and the highest protein yield came from

growth for 24 h without addition of Iptg. It has been previously shown that high levels of protein production can be obtained in stationary phase for cells grown in the absence of inducer (*20*). The two-step purification procedure allowed for high yields of homogeneous, stable, and active enzyme.

Analytical gel filtration and dynamic light scattering experiments indicate that AAC(3)-IV is present as a dimer in solution. These data differ from previous results where it was suggested that AAC(3)-IV is monomeric in the presence of 6 mM 2-mercaptoethanol (*18*). It is possible that the dimer we observe is linked by disulfide bonds, as we have not included thiol reducing agents in our preparation, which would interfere with the spectrophotometric assay. ITC experiments revealed that there is one substrate-binding site per monomer. We suggest that AAC(3)-IV exists as a dimer containing two active sites.

Steady-state kinetic parameters were determined for a number of acyl-donors and aminoglycosides (Table 1). Acetyl-CoA is the strongly preferred acyl donor, as revealed by the determined k_{cat}/K_m, which decrease as the acyl group becomes larger. The effect for propionyl-CoA is predominantly a K_m effect with little alteration on k_{cat}, however butyryl-CoA shows significant effects on both k_{cat} and K_m. An even more dramatic decrease on k_{cat}/K_m is observed with malonyl-CoA as the acyl donor. This narrow specificity with respect to the acyl-CoA substrate has also been reported for other *N*-acetyltransferases (*5, 15*), and suggests a sterically restricted acyl coenzyme A binding site that influences both binding and catalysis.

In contrast to its narrow acyl donor specificity, AAC(3)-IV has an expansive substrate specificity with respect to aminoglycosides. Of all the AAC(3)s described to date (types I (*5*), II (*6*), and III (*7*)), AAC(3)-IV has the broadest range. All aminoglycosides tested in this study were substrates for this enzyme, including the atypical aminoglycoside apramycin, which is a substrate for only two aminoglycoside *N*-acetyltransferases described so far, AAC(3)-IV and AAC-(1) (*21*).

The 1-*N*-acylated aminoglycosides butirosin, amikacin, and netilmicin showed a dramatic reduction in activity when compared to their nonacylated analogues, ribostamycin, kanamycin A, and sisomycin, respectively (Table 1). Similar results have been observed in studies with other aminoglycoside 3-*N*-acetyltransferases, including AAC(3)-III (*7*) and AAC(3)-I (*5*). Acylation at the 1-*N* position has been suggested to sterically interfere with 3-*N* acetylation. In support of this notion, the 1-*N* ethyl group of netilmycin (Figure 1) causes a decrease of 200-fold on its k_{cat}/K_m value in comparison to sisomycin. However, the bulkier 1-*N* hydroxybutyramide groups of amikacin and butirosin (Figure 1) cause a decrease of 750- and 3000-fold, respectively, on their k_{cat}/K_m values compared to kanamycin and ribostamycin.

AcCoA-dependent acetyltransferases are known to use two distinct mechanisms to catalyze the acetyl transference. One mechanism involves the transfer of the acetyl group from AcCoA to an enzyme side chain and then to the amine, or acyl acceptor, substrate. The second mechanism involves direct acetyl transfer from AcCoA to the amine substrate with the formation of a tetrahedral intermediate. The latter mechanism requires that both substrates and enzyme must form a ternary complex before catalysis can occur. To distinguish between a ternary complex (sequential) and covalent-intermediate formation (ping-pong mechanism), initial velocity studies were performed with AcCoA and ribostamycin. The intersecting initial velocity pattern (Figure 2) suggests a sequential kinetic mechanism, where both substrates must bind to the enzyme before catalysis can occur. This mechanism has been shown to be universal for all aminoglycoside *N*-acetyltransferases studied to date.

Dead-end inhibition studies were carried out to determine the order of substrate binding to AAC(3)-IV (Table 2, Figure S2). In the case of most aminoglycoside *N*-acetyltransferases, the order of substrate binding is either random (*15, 17, 22*) or ordered with AcCoA binding first, followed by the aminoglycoside (*14, 23*). AAC(3)-IV exhibited competitive dead-end inhibition for desulfo-CoA versus acetyl-CoA and noncompetitive inhibition versus ribostamycin. When butirosin was used as the inhibitor, competitive inhibition was observed versus ribostamycin and noncompetitive inhibition versus AcCoA. These results are compatible with a random binding of the substrates to the enzyme.

To confirm the binding of both AcCoA and aminoglycoside to the free enzyme, we performed ITC experiments (Figure S5, Table 3). Both AcCoA and ribostamycin are able to bind to the free enzyme, supporting the random binding of substrates to AAC(3)-IV. The ITC data allow the enthalpic and entropic contributions to binding to be dissected. AcCoA binding is highly enthalpically driven, with a modest entropic compensation. In stark contrast, ribostamycin binding is nearly completely entropically driven. These data are quite different from data reported for the AAC(6′)-Iy *N*-acetyltransferase (*24*) and highlight the differences between AAC-(3)-IV and the aminoglycoside acetyltransferases that are members of GNAT superfamily.

Deviations from the Michaelis−Menten kinetics have been frequently observed in systems that employ a random mechanism for binding of substrates. In the case of aminoglycoside *N*-acetyltransferases, Northrop has reported such behavior for gentamicin acetyltransferase I (*17*).

It has been theoretically demonstrated (*25*) that such deviations can be considered to arise from a competition between the two substrates for the free enzyme. This means that substrate inhibition or substrate activation arises due to a shift of the preferred pathway for the ternary complex formation. In such cases, nonlinearity in Lineweaver−Burk plots with respect to one substrate can be completely eliminated by increasing the concentration of the second substrate (*25*).

In the case of AAC(3)-IV, substrate inhibition can be observed at high aminoglycoside concentrations, as can substrate activation, and these are influenced by the fixed concentration of AcCoA (Figure S4, Supporting Information). Taken together, all these data support a random kinetic mechanism (Scheme 2), with the preferred order of substrate binding based on the affinity of the substrate for the enzyme and the cosubstrate concentration.

The determination of the pH dependence of the maximum velocity (Figure 3) indicates that an ionizable group with a pK_a value of 7.8 ± 0.2 must be deprotonated for optimal acetyltransferase activity. A second ionizable group exhibits a pK_a value of 8.4 ± 0.2 and must be protonated for optimal catalytic efficiency. These enzyme groups likely act as general base and general acid to deprotonate the tetrahedral intermediate and protonate the thiolate anion of the product

Scheme 2: Proposed Kinetic and Chemical Mechanisms for Aminoglycoside Acetylation by AAC(3)-IV

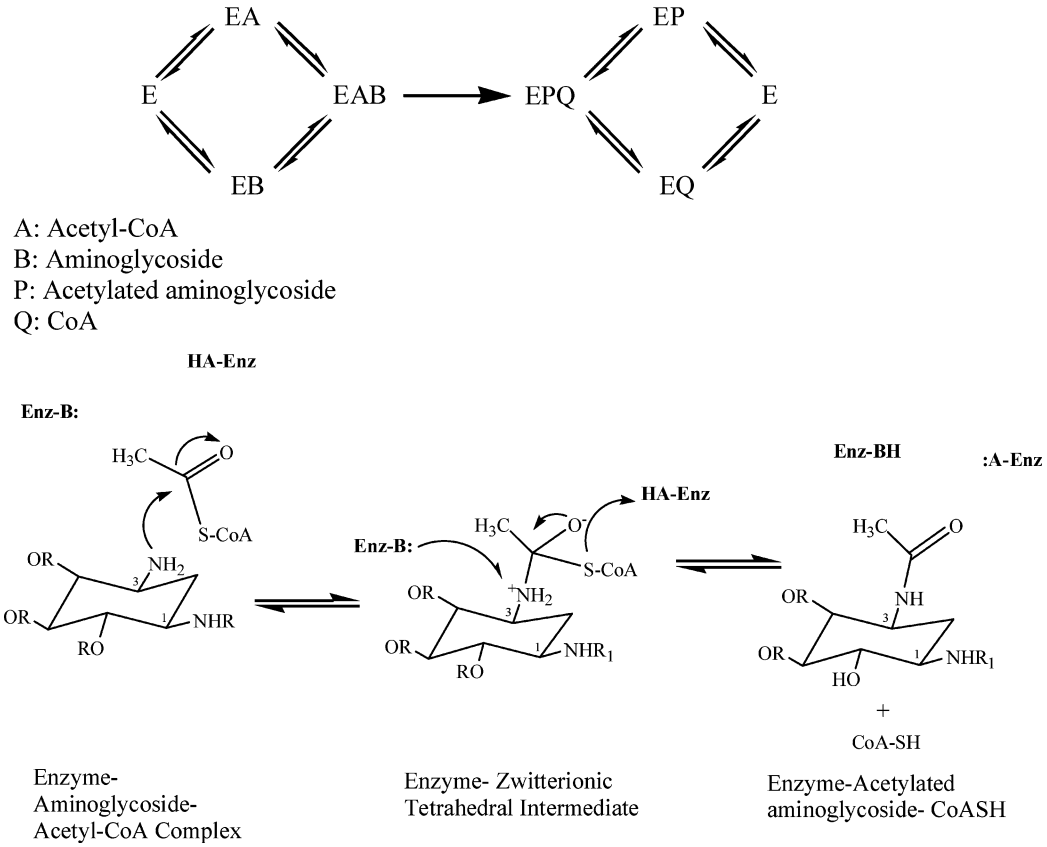

$CoAS^-$, respectively (Scheme 2). The pH dependence of the k_{cat}/K_m plot (Figure 3) revealed two acidic and three basic ionizable groups involved in binding and/or catalysis. Two of these groups are likely to be the same groups observed in the k_{cat} pH profile, while the other three are most likely involved in binding. These groups involved in binding might be enzyme residues or any of the several amino groups present in the aminoglycoside molecule. The nonresolvable pK_a values of 7.2 ± 0.1 and 8.7 ± 0.1 determined from the fit to eq 8 are in the range of pK_a values determined for the amino groups of ribostamycin (Figure 1): 8.6 (6′-NH_2), 7.6 (2′-NH_2), 5.7 (3-NH_2), and 8.1 (1-NH_2) (*26*).

To assess the rate-limiting nature of chemical steps, solvent kinetic isotope effects were determined at pH 8.0, a region where the kinetic parameters are relatively independent of small changes in pH (pD) (Figure 4). Solvent kinetic isotope effects were measured by varying the concentration of ribostamycin at a fixed saturating concentration of AcCoA. Identical solvent kinetic isotope effects of 2.5 ± 0.1 were observed on both k_{cat} and k_{cat}/K_m. Equivalent values on $^{D2O}k_{cat}$ and $^{D2O}k_{cat}/K_m$ suggest that one or more proton transfer steps that are an intimate part of the chemical reaction catalyzed by AAC(3)-IV are at least partially rate-limiting in the overall reaction.

The potential for plasmid-encoded and transmissible resistance to essentially all therapeutically useful aminoglycoside antibiotics as a result of expression of AAC(3)-IV enzymes is worrisome. The deoxystreptamine ring that is the core element of aminoglycosides is also the site of acetylation by the enzyme. No detailed mechanistic studies of this enzyme have appeared to date, and no structural information has yet been reported for AAC(3)-IV. The three-dimensional structures of three classes of aminoglycoside *N*-acetyltransferases have been determined (AAC(3)-I, AAC(2′), and two different AAC(6′) isozymes (*27*)), and all exhibit the same fold, however, with distinct differences in the manner in which the catalytically active dimers are generated. The sequence of AAC(3)-IV suggests that it will not adopt the same GNAT fold, raising interesting questions concerning how AcCoA and aminoglycoside substrates are bound to effect regioselective 3-*N*-acetylation. Current efforts are being directed to obtain this structural information.

ACKNOWLEDGMENT

We thank Drs. Tarun K. Dam and C. Fred Brewer for assistance in performing the isothermal titration calorimetry experiments.

SUPPORTING INFORMATION AVAILABLE

Double reciprocal plot of initial rate data at varying ribostamycin and fixed AcCoA concentrations (Figure S1), dead-end inhibition patterns (Figure S2), solvent kinetic isotope effect determined for AAC(3)-IV (Figure S3), deviations of the Michaelis−Menten kinetics at high sisomycin concentrations (Figure S4), and ITC profiles of AAC(3)-IV with ribostamycin and with AcCoA (Figure S5). This material is available free of charge via the Internet at http://pubs.acs.org.

REFERENCES

1. Davies, J., and Wright, G. D. (1997) Bacterial resistance to aminoglycoside antibiotics, *Trends Microbiol. 5*, 234−240.
2. Mingeot-Leclercq, M. P., Glupczynski, Y., and Tulkens, P. M. (1999) Aminoglycosides: activity and resistance, *Antimicrob. Agents Chemother. 43*, 727−737.

3. Llano-Sotelo, B., Azucena, E. F., Jr., Kotra, L. P., Mobashery, S., and Chow, C. S. (2002) Aminoglycosides modified by resistance enzymes display diminished binding to the bacterial ribosomal aminoacyl-tRNA site, *Chem. Biol. 9*, 455−463.
4. Magnet, S., and Blanchard, J. S. (2005) Molecular insights into aminoglycoside action and resistance, *Chem. Rev. 105*, 477−498.
5. Williams, J. W., and Northrop, D. B. (1978) Substrate specificity and structure-activity relationships of gentamicin acetyltransferase I. The dependence of antibiotic resistance upon substrate Vmax/Km values, *J. Biol. Chem. 253*, 5908−5914.
6. Le Goffic, F., Martel, A., and Witchitz, J. (1974) 3-N enzymatic acetylation of gentamicin, tobramycin, and kanamycin by Escherichia coli carrying an R factor, *Antimicrob. Agents Chemother. 6*, 680−684.
7. Biddlecome, S., Haas, M., Davies, J., Miller, G. H., Rane, D. F., and Daniels, P. J. (1976) Enzymatic modification of aminoglycoside antibiotics: a new 3-N-acetylating enzyme from a Pseudomonas aeruginosa isolate, *Antimicrob. Agents Chemother. 9*, 951−955.
8. Davies, J., and O'Connor, S. (1978) Enzymatic modification of aminoglycoside antibiotics: 3-N-acetyltransferase with broad specificity that determines resistance to the novel aminoglycoside apramycin, *Antimicrob. Agents Chemother. 14*, 69−72.
9. Chaslus-Dancla, E., Martel, J. L., Carlier, C., Lafont, J. P., and Courvalin, P. (1986) Emergence of aminoglycoside 3-N-acetyltransferase IV in Escherichia coli and Salmonella typhimurium isolated from animals in France, *Antimicrob. Agents Chemother. 29*, 239−243.
10. Chaslus-Dancla, E., Pohl, P., Meurisse, M., Marin, M., and Lafont, J. P. (1991) High genetic homology between plasmids of human and animal origins conferring resistance to the aminoglycosides gentamicin and apramycin, *Antimicrob. Agents Chemother. 35*, 590−593.
11. Consaul, S. A., and Pavelka, M. S., Jr. (2004) Use of a novel allele of the *Escherichia coli* aacC4 aminoglycoside resistance gene as a genetic marker in mycobacteria, *FEMS Microbiol. Lett. 234*, 297−301.
12. Bradford, M. M. (1976) A rapid and sensitive method for the quantitation of microgram quantities of protein utilizing the principle of protein-dye binding, *Anal. Biochem. 72*, 248−254.
13. Wiseman, T., Williston, S., Brandts, J. F., and Lin, L. N. (1989) Rapid measurement of binding constants and heats of binding using a new titration calorimeter, *Anal. Biochem. 179*, 131−137.
14. Hegde, S. S., Javid-Majd, F., and Blanchard, J. S. (2001) Overexpression and mechanistic analysis of chromosomally encoded aminoglycoside 2′-N-acetyltransferase (AAC(2′)-Ic) from Mycobacterium tuberculosis, *J. Biol. Chem. 276*, 45876−45881.
15. Magnet, S., Lambert, T., Courvalin, P., and Blanchard, J. S. (2001) Kinetic and mutagenic characterization of the chromosomally encoded Salmonella enterica AAC(6′)-Iy aminoglycoside N-acetyltransferase, *Biochemistry 40*, 3700−3709.
16. Coombe, R. G., and George, A. M. (1982) Purification and properties of an aminoglycoside acetyltransferase from Pseudomonas aeruginosa, *Biochemistry 21*, 871−875.
17. Williams, J. W., and Northrop, D. B. (1978) Kinetic mechanisms of gentamicin acetyltransferase I. Antibiotic-dependent shift from rapid to nonrapid equilibrium random mechanisms, *J. Biol. Chem. 253*, 5902−5907.
18. Brau, B., and Piepersberg, W. (1985) Purification and characterization of a plasmid-encoded aminoglycoside-(3)-N-acetyltransferase IV from Escherichia coli, *FEBS Lett. 185*, 43−46.
19. Wolf, E., Vassilev, A., Makino, Y., Sali, A., Nakatani, Y., and Burley, S. K. (1998) Crystal structure of a GCN5-related N-acetyltransferase: Serratia marcescens aminoglycoside 3-N-acetyltransferase, *Cell 94*, 439−449.
20. Magalhaes, M. L., Pereira, C. P., Basso, L. A., and Santos, D. S. (2002) Cloning and expression of functional shikimate dehydrogenase (EC 1.1.1.25) from Mycobacterium tuberculosis H37Rv, *Protein Expression Purif. 26*, 59−64.
21. Lovering, A. M., White, L. O., and Reeves, D. S. (1987) AAC(1): a new aminoglycoside-acetylating enzyme modifying the Cl aminogroup of apramycin, *J. Antimicrob. Chemother. 20*, 803−813.
22. Radika, K., and Northrop, D. B. (1984) The kinetic mechanism of kanamycin acetyltransferase derived from the use of alternative antibiotics and coenzymes, *J. Biol. Chem. 259*, 12543−12546.
23. Draker, K. A., Northrop, D. B., and Wright, G. D. (2003) Kinetic mechanism of the GCN5-related chromosomal aminoglycoside acetyltransferase AAC(6′)-Ii from Enterococcus faecium: evidence of dimer subunit cooperativity. *Biochemistry 42*, 6565−6574.
24. Hegde, S. S., Dam, T. K., Brewer, C. F., and Blanchard, J. S. (2002) Thermodynamics of aminoglycoside and acyl-coenzyme A binding to the Salmonella enterica AAC(6′)-Iy aminoglycoside N-acetyltransferase, *Biochemistry 41*, 7519−7527.
25. Pettersson, G. (1977) Substrate-inhibition and substrate-activation in the random-order ternary-complex mechanism for enzyme reactions involving two substrates, *Biochim. Biophys. Acta 484*, 199−207.
26. Xin-Shan, Y., and Zhang, L. H. (2002) Aminoglycoside mimetics as small-molecule drugs targeting RNA, *Curr. Med. Chem. 9*, 929−939.
27. Vetting, M. W., de Carvalho, L. P. S., Yu, M., Hegde, S. S., Magnet, S., Roderick, S. L., and Blanchard, J. S. (2005) Structure and functions of the GNAT superfamily of acetyltransferases, *Arch. Biochem. Biophys. 433*, 212−226.

BI051777D